

## Article

# Sex Recognition through ECG Signals aiming toward Smartphone Authentication

Jose-Luis Cabra Lopez <sup>1,\*</sup> , Carlos Parra <sup>2</sup>, Libardo Gomez <sup>1</sup> and Luis Trujillo <sup>2</sup>

<sup>1</sup> Department of Telecommunications, Faculty of Engineering, Fundación Universitaria Compensar, Bogota 111311, Colombia; lgomezd@ucompensar.edu.co

<sup>2</sup> Department of Electronics, Faculty of Engineering, Pontificia Universidad Javeriana, Bogota 110231, Colombia; carlos.parra@javeriana.edu.co (C.P.); trujillo.luis@javeriana.edu.co (L.T.)

\* Correspondence: jlcabra@ucompensar.edu.co; Tel.: +57-311-822-86-36

**Abstract:** Physiological signals are strongly related to a person's state of health and carry information about the human body. For example, by ECG, it is possible to obtain information about cardiac disease, emotions, personal identification, and the sex of a person, among others. This paper proposes the study of the heartbeat from a soft-biometric perspective to be applied to smartphone unlocking services. We employ the user heartbeat to classify the individual by sex (male, female) with the use of Deep Learning, reaching an accuracy of  $94.4\% \pm 2.0\%$ . This result was obtained with the RGB representation of the union of the time-frequency transformation from the pseudo-orthogonal X, Y, and Z bipolar signals. Evaluating each bipolar contribution, we found that the XYZ combination provides the best category distinction using GoogLeNet. The 24-h Holter database of the study contains 202 subjects with a female size of 49.5%. We propose an architecture for managing this signal that allows the use of a few samples to train the network. Due to the hidden nature of ECG, it does not present vulnerabilities like public trait exposition, light/noise sensibility, or learnability compared to fingerprint, facial, voice, or password verification methods. ECG may complement those gaps en route to a cooperative authentication ecosystem.

**Keywords:** sex recognition; ECG; user authentication; soft-biometrics; smartphone applications; machine learning



**Citation:** Cabra Lopez, J.-L.; Parra, C.; Gomez, L.; Trujillo, L. Sex Recognition through ECG Signals aiming toward Smartphone Authentication. *Appl. Sci.* **2022**, *12*, 6573. <https://doi.org/10.3390/app12136573>

Academic Editors: Jongweon Kim and Yongseok Lee

Received: 14 May 2022

Accepted: 23 June 2022

Published: 29 June 2022

**Publisher's Note:** MDPI stays neutral with regard to jurisdictional claims in published maps and institutional affiliations.



**Copyright:** © 2022 by the authors. Licensee MDPI, Basel, Switzerland. This article is an open access article distributed under the terms and conditions of the Creative Commons Attribution (CC BY) license (<https://creativecommons.org/licenses/by/4.0/>).

## 1. Introduction

ECG signals are mostly used for monitoring a patient's health status. This signal can provide information about arrhythmia and coronary artery disease, among other conditions. However, researchers have found that it is possible to extract from the heartbeat specific information such as emotions [1], age estimation [2], person identification [3], and sex [4].

Sex recognition has been studied using body [5] and face [6] images, gait [7], voice [8], twittering [9], and keystroke dynamics [10], among others.

Cardiovascular diseases are the most prominent cause of death in the world [11]. According to the Centers for Disease Control and Prevention, each year in the USA, around 659,000 people die from heart failure, which represents 25% of deaths in the country [12]. At approximately 65 and 72 years old, respectively, men and women suffer their first heart attack [13]. Some studies have shown that men are twice as susceptible to having a heart attack as women [14,15], though the survival rate after a heart attack is lower in women [13]. This may be attributed to the fact that a woman's heart tends to be smaller and can pump 10% less blood, and potentially because women experience the heart attack at an older age [16]. Women's hearts tend to have shorter PR and QRS intervals [17], longer QT duration, and distinct T waveform dynamics compared to men [18].

We propose the ECG sex classification study as the first step and approach to fighting cardiovascular diseases because the discrimination could help to emphasize specific heart

behaviors given the person's anatomical features. Although sex recognition has been covered by cardiologists, this area has turned to machine learning (ML) algorithms since 2014 [3,19], and reciprocally, ECG has proven its biometric characteristics through ML, too [20].

In fact, biometric multimodal studies have pointed out that the inclusion of soft-biometric features can enrich and facilitate the discrimination performance [21], being mostly proven in camera-related systems. Soft-biometric refers to the extraction of shared—or nonunique—traits such as ethnicity, sex, age, etc., that help to describe human subjects but are not strong enough to distinguish between two people [22]. Following this scheme, we propose to treat the ECG sex property as a soft-biometric input for future inclusion in ECG-related verification engines to complement the classification space. Moreover, we intend to strengthen this technology to be adapted as a smartphone authentication tool in the near future. Recent tests show that smartphone fingerprint and face authentication hacking is possible [23–26], evidencing that biometric authentication is not infallible [27]. Therefore, user privacy protection should be turned into an authentication community, embracing possible traits that could support the current open gates. In consequence, it is necessary to be aware of the strengths and weaknesses of authentication tools when the user context changes because each biometric method assumes the sensor's constraints. ECG biometrics' potential is not affected by light-saturated or noisy environments in contrast to touch-screen, camera, or microphone sensors. In addition, due to the face exposition or the fingerprint trace in daily touched objects, the copy reproduction attack is more probable for face and fingerprint. Instead, ECG is a hidden measure [3]. The nature of ECG includes an inherent liveness property as a prospective ubiquitous tool that could be used for continuous or transparent authentication mechanisms. Although this area is still maturing, dealing with issues such as signal time acquisition, computational complexity, and user comfortability, new related products evidence the first market inclusions as described in Section 5.

The ECG fiducials orientation finds the temporal and amplitude inter- and intra-proportions of the P, Q, R, S, and T peaks (Figure 1) and has been a classical and useful tool for studying the ECG. However, fiducial-based approaches do not cover all the signal waveform; for that reason, it is preferable to choose transformations or feature extraction options that can completely cover the heartbeat. On the other hand, intending to develop a portable device, variables such as comfort and fast configuration require a fewer amount of electrodes; nevertheless, the best accuracy scores in sex recognition mostly implement a 12-lead configuration using deep learning as a classifier. Similarly, during the day, a person's stance directly affects the heartbeat waveform change; indeed, in the field of sex recognition, resting position samples have a preponderance in several studies. Moving to the smartphone authentication space, users demand a fast process for unlocking their devices; in contrast, ten seconds is the common window in the related work. Finally, unlike static biometric traits such as face or fingerprint, the heart contains a dynamic behavior, so the classifier needs to consider and adopt its conditions to the nature of this phenomenon.

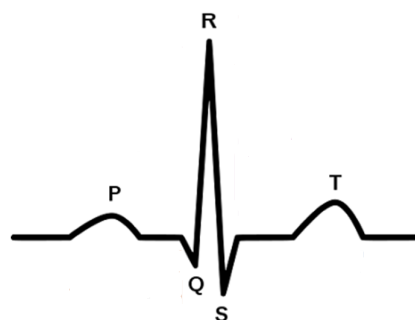


**Figure 1.** Fiducial PQRST. Based on [28].

In the next list, we show the series of contributions of this text.

1. We implement a novel system that uses heart rate as a feature of a classifier selection, reaching a general accuracy of  $94.4\% \pm 2.0\%$  with a peak over 96% in some bins, collecting only four heartbeats per sample.
2. Our approach does not use the 12-lead configuration that is common in related studies. In contrast, we implement the use of pseudo-orthogonal lead configuration that uses three signals.
3. We propose an RR discrimination to feed the Deep Convolutional Neural Network (CNN) classifier. It provides a fewer number of samples to train the classifier but achieves similar results compared with related work.
4. Taking advantage of all the signal waveforms, we provide an RGB strategy for representing orthogonal lead signals in one sample through a wavelet transform.
5. Our experiment can classify the person's sex without controlling the person's stance.

The structure of this work starts with the related work on sex classification in Section 2, providing the last results in this area. The section of materials and methods are covered in Section 3.1 with the database features, and Section 3.2 covers the methodology proposed in this work. Then, in Section 4, we expose the architecture that contains the procedure implemented in our work. The experimental results are exposed in Section 5, and lastly, we conclude this article with our final discussion (Section 6) and conclusions (Section 7) of the topics mentioned in this text.

## 2. Related Work

This section intends to provide a scope of the work on sex recognition in ECG during the last few years, starting with an overview of Deep Learning in ECG, covering some examples of applications such as arrhythmias, sleep apnea, pregnancy, R peak detection, QRS complex recognition, cardiac rhythm, and human identification.

Most of the work in Deep Learning in ECG is related to arrhythmia detection with the intention of avoiding human errors and supporting the processing of large databases for better diagnosis. Izci et al. with a CNN and the database MIT-BIH differentiate normal beats of left bundle branch block (LBBB), right bundle branch block (RBBB), premature ventricular contractions (PVC), and premature atrial contractions (PAC) arrhythmias with a 98.07% of accuracy [29]. Essa et al. [30], following arrhythmia detection, proposed the bagging model of a CNN-LSTM (long short-term memory) and RRHOS-LSTM (RR Interval and higher-order statistics) classifiers, each trained with different sub-samples, being both connected with an ANN meta-classifier and verified with a final CNN-LSTM model, allowing a general performance of 95.81%. Ahmad et al. [31] proposed the Multimodal Image Fusion (MIF) and the Multimodal Feature Fusion (MFF) frameworks for arrhythmia and Myocardial Infarction, each receives the ECG signal transformed into Gramian Angular Field, Recurrence Plot, and Markov Transition Field images. MIF creates a new image fusing its image input for CNN classification, while MFF generates the fusion of the extracted features of the CNN penultimate layer for training a Support Vector Machine (SVM) for heartbeat classification. Finally, the model got an accuracy of 99.7% and 99.2% for arrhythmia and Myocardial Infarction. Jinghao et al. [32], from an inter-patient perspective, transform the signal waveform and dynamics into a symbolic space in the MIT-BIH arrhythmia dataset to detect the supraventricular ectopic beat (SVEB) and ventricular ectopic beat (VEB) using a multiperspective convolutional neural network with an overall accuracy of 96.4%. Due to the extension of this field, Ebrahimi et al. [33] composed a review focused on the application of deep learning for the detection of arrhythmias.

Covering the sleep apnea detection study, Bahrami et al. [34] performed a comprehensive comparison between 14 conventional ML algorithms and deep learning approaches such as CNN, recurrent networks, and hybrid-CNN, having the best detection on hybrid deep models with an accuracy, sensitivity, and specificity of 88.13%, 84.26%, and 92.27%. For pregnancy ECG separation, Lee et al. [35] seek to distinguish the ECG of the prenatal person due to the dominance of the abdominal maternal ECG signal, looking for early cardiac detection risks, decomposing the joint signal using the W-net deep learning architecture based

on QRS complexes with a recall and precision of 98.23% and 99.3% with the abdominal and direct fECG database (ADFECGDB). For future analysis, there is an approach proposed by Li et al. to be tested that consists of the signal separation by IMF decomposition to recognize specific maternal and prenatal components by LSTM-RNN [36,37]. In the R peak detection, the study of Gajare et al. is trained with wavelet scalograms from the ECG Heartbeat Categorization Dataset from Kaggle and evaluated by the MIT-BIH Arrhythmia Dataset, achieving an accuracy of 98.32% [38]. In the field of QRS findings, Cai et al. [39], with the presence of noise in arrhythmia samples, categorize it with CNN and CRNN models, reaching an F1 score of 0.99 with four different databases, ensuring a generalizable model. Pokaprakarn et al. [40] classify the ECG rhythm with the spectrogram and signal waveform inputs with sequences of 5 seconds with noise presence and verified it with an external database, achieving an F1 score of 0.89 for discriminating Normal Sinus Rhythm (NSR), Atrial Fibrillation (AF), Supraventricular Tachyarrhythmia (SVTA), Bigeminy (B), and Trigeminy (T) classes. Finally, an emerging area is biometric ECG. An application example is performed by Abdeldayem et al., which developed a person identification CNN classification cross-validating nine different databases reaching a 95.6% accuracy in extracting attributes by spectral correlation [41]. Due to the expansion of this topic, we recommend the work of Uwaechia et al. [42], which presents a survey that covers deep supervised learning, deep semi-supervised learning, and deep unsupervised learning methods for the identification of people.

Regarding ECG sex recognition, Strodtzoff et al. provided the Physikalisch-Technische Bundesanstalt (PTB-XL), a database that contains 71 different annotations and 5 diagnostic super-classes. PTB-XL follows the standard communications protocol for computer-assisted electrocardiography (SCP-ECG) with the purpose of being a reference point for future research into the machine learning scope for different classification approaches in ECG [43]. Additionally, they seek to classify person sex with transfer learning and inception models, getting an accuracy of 84.9% with a ResNet pre-trained model. Strodtzoff et al.'s work also focuses their direction on age prediction, diagnosis likelihood, and person stratification.

The work proposed by Siegersma et al. used a study of risk mortality by misclassified sex data with an increasing score of 1.4 times over people with ECG samples that were properly classified [44]. At the same time, they implemented a Deep Neural Network (DNN) for sex classification, achieved an interval confidence of 95%, an accuracy score of 89% for internal validation, and [80%, 82%] and [80%, 83%] for external validation, using two different databases.

On the other hand, Diamant et al., based on SimCLR [45], implemented a system that automatically acquires information about the ECG signal for a pre-training stage known as PCLR, trained with around 3.2 million ECGs, using contrastive learning without the requirement to fine-tune the network [46]. They transform each sample into a lineal representation, and contrastive learning allows a self-supervised scheme for data without annotations that focuses on highlighting regions with similarity or distinction to be usable in new operations. The system focuses on age prediction, sex classification, and left ventricular hypertrophy (LVH) and atrial fibrillation (AF) detection passed through four steps: selection module, encoder, projection head, and contrastive loss function. For sex classification, with more than 5000 samples, it achieves an F1 score of 86%.

It is also noteworthy that the contributions of Attia et al. [2], Siegersma et al. [4], and Lyle et al. [47] reached accuracies of 90.4%, 92.2%, and [91.3%, 86.3%], respectively. In Table 1, more indicators can be found regarding the mentioned work in this section.

The advantage of our work in comparison with the related work is the significant accuracy score, taking into account variables such as: (i.) A minor number of electrodes on the person represents less complexity in the installation, increasing the user comfort. (ii.) Fewer signals to study. (iii.) Minor signal window acquisition. (iv.) Proposal of signal integration (v.) The nature of our analyzed database and our work classifies sex without taking into account the person's stance, while the related work mostly works with patients in resting position.

**Table 1.** Related work about ECG sex identification with ML algorithms.

Ref.	Acc. [%]	Lead	Sample Length [s]	Tech.	Fs [Hz]	Position	Male-Female [%]	Tr.   Ts. Sample	Year
[2]	90.4	12	10	CNN	500	Supine	52–48	~500 k   ~275 k	2019
[4]	92.2	12	N/A	DNN	N/A	N/A	50.5–49.5	~131 k   ~68.5 k	2021
[47]	DB1: 91.3 DB2: 86.3	12	10	SPAR & KNN	DB1: 1000 DB2: 500	Resting	DB1: 60–40 DB2: 46–54	DB1: N = 0.104 k DB2: N = 8.9 k	2021
[43]	84.9	12	10	CNN xresnet 1d101	100	Resting	52–48	N = ~22 k 10 fold: 8   2	2021
[44]	valid. int: 89 ext: 81 & 82	12	10	DNN	250 or 500	Resting	Tr: N/A int. valid.: N/A ext. valid. 42.6–57.4	Tr: ~132 k int. valid.: 68.5 k ext. valid.: 7.7 k	2022
[46]	f-score: 87	12	10	PCLR & contrastive learning	250 or 500	Resting	N/A	N = ~3229 k 90%   10%	2022
Own	94.4	6	3.93	CNN	200	Random	51–49	~3 k   ~1.3 k	2022

### 3. Materials and Methods

#### 3.1. Database Features

Our data belongs to the medical center of the University of Rochester with the code reference E-HOL-03-0202-003 [48]. It includes 202 healthy patients using a pseudo-orthogonal lead configuration (X, Y, and Z) acquired from a 24-h Holter. Only heartbeats labeled as Normal are used in this research. Complementing the official statistics, we have detected four things: (1.) All labels, such as R peak location, start after minute 5. (2.) The mean recording duration is  $19.7 \pm 6.1$  h. (3.) Thew’s website informs us that there are two sex labels marked as unknown; this information is incorrect, and the University of Rochester confirms that there are 102 Males and 100 Females. (4.) We decided to ignore volunteer #1043 due to quality issues.

The pseudo-orthogonal placement intends to capture the heart signal from three orthogonal vectors, using six electrodes for acquiring the bipolar signals X, Y, and Z, following Figure 2. The X signal is achieved at the V6 position with its right equivalent point. The Y signal starts in the left anterior axillary line at the lower rib until the upper sternum. Finally, the Z signal is at the V3 position, both frontal and on the person’s back.

#### 3.2. Methodology

Looking to cover the heartbeat dynamism, we adapt the histogram strategy to see the differences between male and female heartbeats based on their rhythm. Commonly, the RR interval oscillates from 0.6 to 1.2 s [50]. In this way, we defined the border values of the histogram. Then, with a bin width of 0.06 seconds, the total number of bins is ten. This value is calculated from the difference between the maximum and minimum values in the dataset divided by the width of the bin. Figure 3, with 9 million samples for each sex, helps to establish that both categories (male and female) possess similar RR tendencies, separated into 10 bins with seconds as the unit.

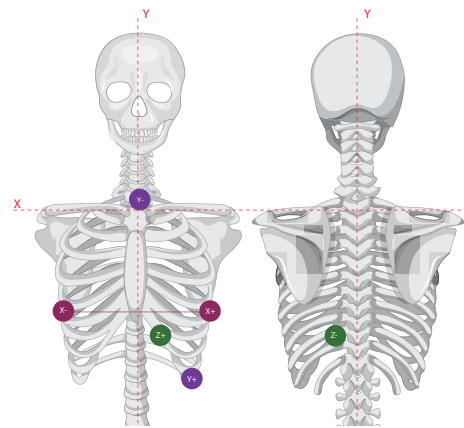


Figure 2. Pseudo-orthogonal lead configuration. Based on [49].

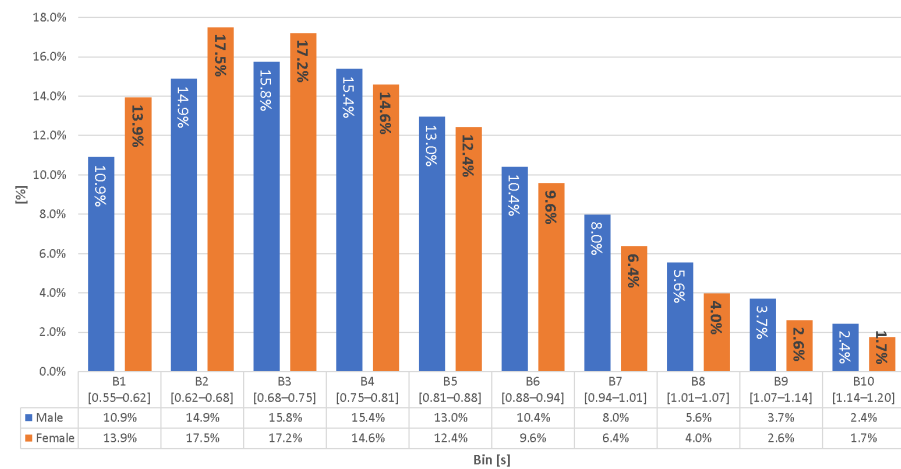


Figure 3. Heart rate histogram by sex—10 bins.

Taking advantage of the previous distribution, we propose to discriminate each bin into a different classification model (Figure 4). This is to better differentiate the set of heartbeats. We assume that similar RRs have similar waveforms with the intention of helping the classifier performance.

With the purpose of evaluating each signal input, we will develop the same experiment structure seven times but enable the ECG signal leads in different moments. As a result, the set of experiments will have the following sequence X, Y, Z, XY, XZ, YZ, XYZ.

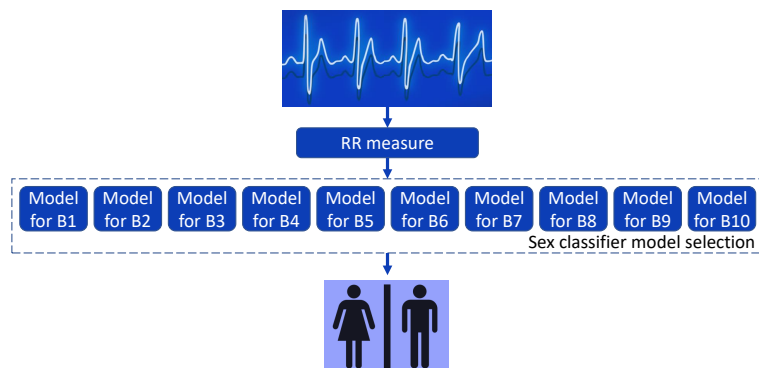


Figure 4. Heartbeat study methodology.

#### 4. Architecture

An overview of the scheme proposed in this work consists of six blocks described in Figure 5. (i.) The database module contains the set of ECG data to analyze with the

attributes described in Section 3.1. (ii.) The noise filtering component implements both high- and stop-band filtering over the X, Y, and Z signals. (iii.) The heartbeat selector block collects each heartbeat separately oriented by the ten bins in Figure 3 and randomly selects two of them, each composed of four beats. (iv.) The signal transformation module uses each four-beat sample composed of the X, Y, and Z signals and turns each into the time-frequency domain to build the RGB image. (v.) The samples storage element collects each image, saving it in the folder male or female, as appropriate. (vi.) The classification section generates the computational model; for this, it distributes and processes the storage samples' data for the training and testing of the model.

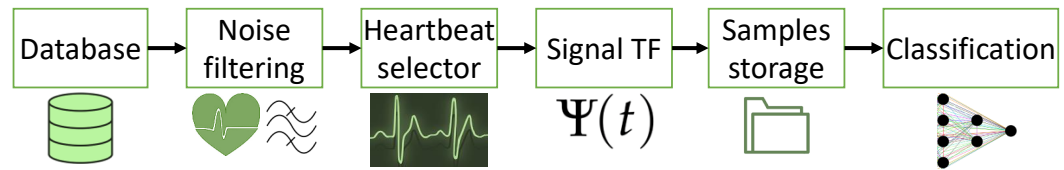


Figure 5. System block diagram.

Delving into the scheme of Figure 5, we propose that the architecture described in Figure 6 is composed of two general moments: signal preprocessing and data classification. The next procedure is applied to each person in the database.

The preprocessing stage contains five moments, taking into account that the signals X, Y, and Z are involved in each step. To start, the complete recording goes through a high-pass filter of 0.7 Hz and a notch filter of 50/60 Hz to remove noises such as baseline wander and powerline. Then, taking advantage of the database annotations in the Holter recording (Section 3.1), we collected the vector indices of common RR values according to their working bin (Figure 3). Consequently, by RR value, we randomly take two of them, including their next three R peaks, to complete one sample.

For the next step, the X, Y, and Z samples are transformed into the wavelet space. This transformation helps to exploit the entire ECG waveform, highlighting jointly both time and frequency data in a two-dimensional space without data loss. We have implemented a continuous wavelet filter-bank that follows an analytic Morse wavelet with a time-bandwidth product of 60, a symmetry characterization of 3, and a voice per octave of 12.

Each matrix transformation magnitude (Wvt-X, Wvt-Y, Wvt-Z) is used as a part of an RGB image. That is to say, the matrices Wvt-X, Wvt-Y, and Wvt-Z each correspond to the colors red, green, and blue, in strict order; if required, a zero matrix is used as a replacement when the X, Y, or Z leads are disabled. Finally, each image is stored in a different folder, depending on the person's sex.

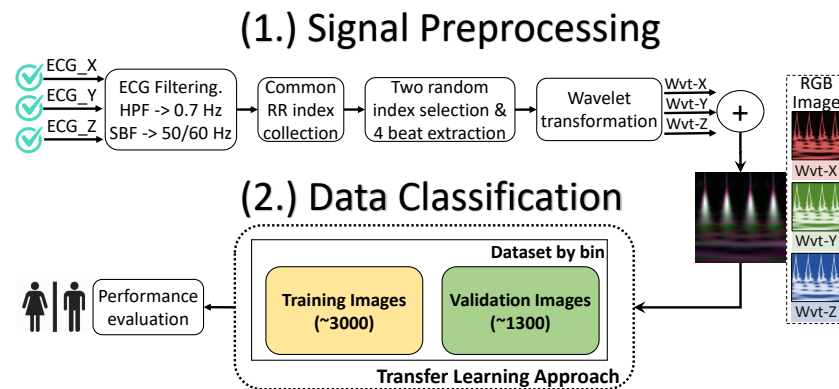


Figure 6. Research architecture.

The classification is performed with a data distribution of 70–30%. We decided to use a pre-trained network called GoogLeNet, which is a convolutional neural network of 144

layers provided by Google. The network dropout implemented is 60%, a minibatch size of 15 samples, and a maximum number of epochs of 20.

### 5. Results

We show seven different and independent experiments following the architecture of Figure 6. We started from single leads (X, Y, Z), then with the possible set of combinations (XY, XZ, YZ, XYZ). The results are separated into two parts, single lead and mixed lead analysis.

From the accuracy perspective, X lead reaches an  $87.3\% \pm 4.4\%$ , Y lead  $84.6\% \pm 4.0\%$ , and Z lead  $86.6\% \pm 4.0\%$ . Figure 7 consolidates the results set, and by bin, the biggest score is marked with a red dot. Under bipolar configuration, X lead provides better performance, being positioned in 7 of all 10 bins, compared to Y and Z leads with 1/10 and 2/10, respectively.

Taking only the best results by bin, the general sensitivity climbs to  $89.6\% \pm 4.5\%$ , specificity to  $86.2\% \pm 8.1\%$ , precision to  $86.8\% \pm 6.3\%$ , and the accuracy to  $87.9\% \pm 4.1\%$ . Figure 8 consolidates the confusion matrix derivation results of the classification.

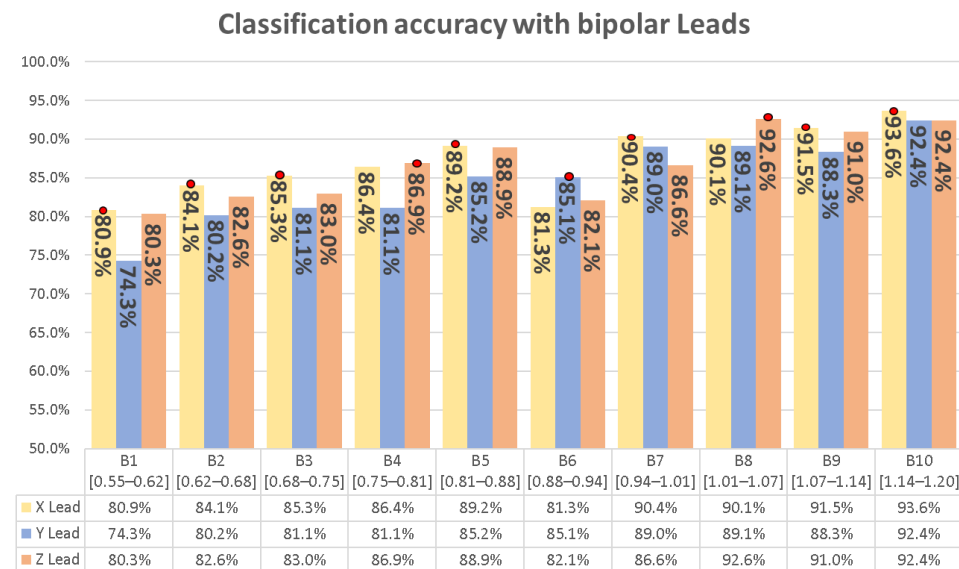


**Figure 7.** Single lead accuracy results. (● means maximum value per set).

On the other hand, the combination of the leads XYZ achieved an accuracy of  $94.4\% \pm 2.0\%$ , which is an improvement of 7.1 points over the bipolar X lead. The XY leads combination achieved an accuracy of  $90.3\% \pm 3.6\%$ , XZ leads  $92.8\% \pm 2.2\%$ , and YZ leads  $89.3\% \pm 2.8\%$ . In 9 of 10 bins, the XYZ signals were the best scheme (Figure 9).

With the best values by bin, the classification rate contains the following results: sensitivity of  $94.4\% \pm 3.6\%$ , specificity of  $94.5\% \pm 3.8\%$ , precision of  $94.4\% \pm 3.4\%$ , and accuracy  $94.4\% \pm 2.0\%$ . The results in Figures 8 and 10 are subtracted from each other and compared in Figure 11. As a result, the sensitivity achieved an advance of [12.7%, 3.5%, 9.7%, 3.6%, 12.0%, 5.6%, 5.5%] in [B1, B3, B4, B6, B7, B9, B10] but a decrement of [1.8%, 2.5%, 0.4%] in [B2, B5, B8]. The specificity achieved an increment of [7.3%, 17.9%, 14.4%, 5.9%, 9.4%, 18.8%, 8.2%, 4.0%] in [B1, B2, B3, B4, B5, B6, B8, B9] but a decrement of [2.1%, 0.9%] in [B7, B10]. The precision achieved an improvement of [7.2%, 14.4%, 12.0%, 6.5%, 9.4%, 15.5%, 8.0%, 4.8%] in [B1, B2, B3, B4, B5, B6, B8, B9] but a decrement of [1.3%, 0.8%] in [B7, B10]. The accuracy in all segments achieved an improvement of [9.9%, 8.2%, 9.0%, 7.8%, 3.5%, 11.3%, 4.8%, 4.1%, 4.7%, 1.9%] in [B1, B2, B3, B4, B5, B6, B7, B8, B9, B10].

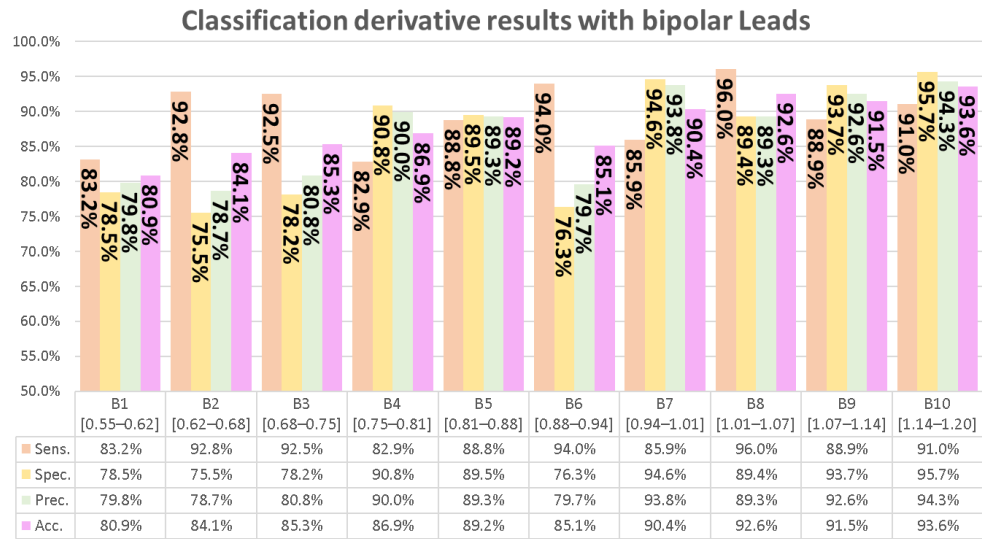


Figure 8. Single lead confusion matrix derivation results.

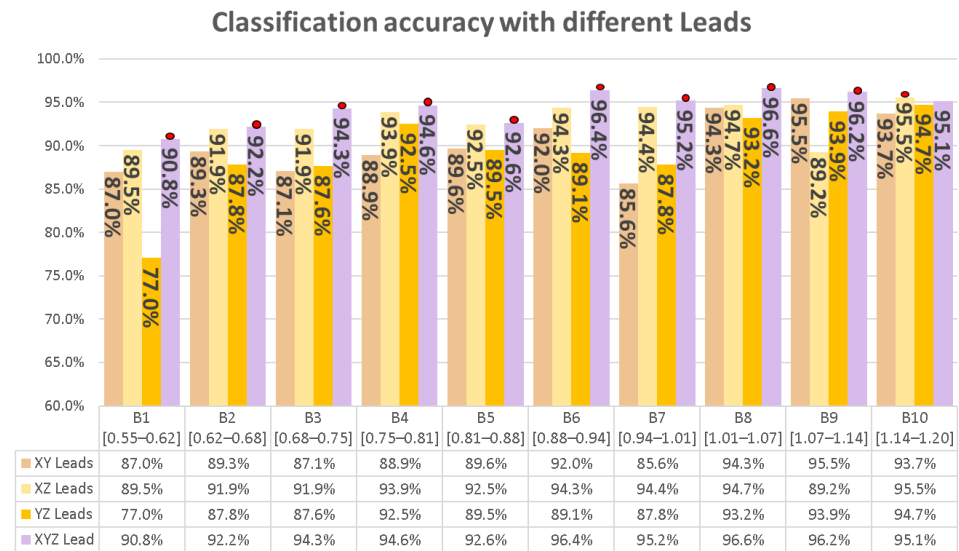


Figure 9. Combined leads accuracy results. (● means maximum value per set).

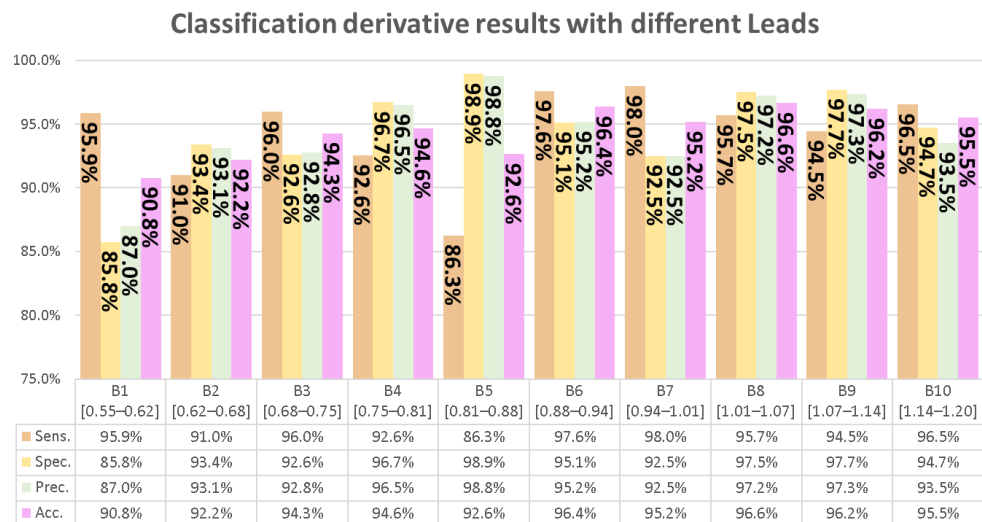
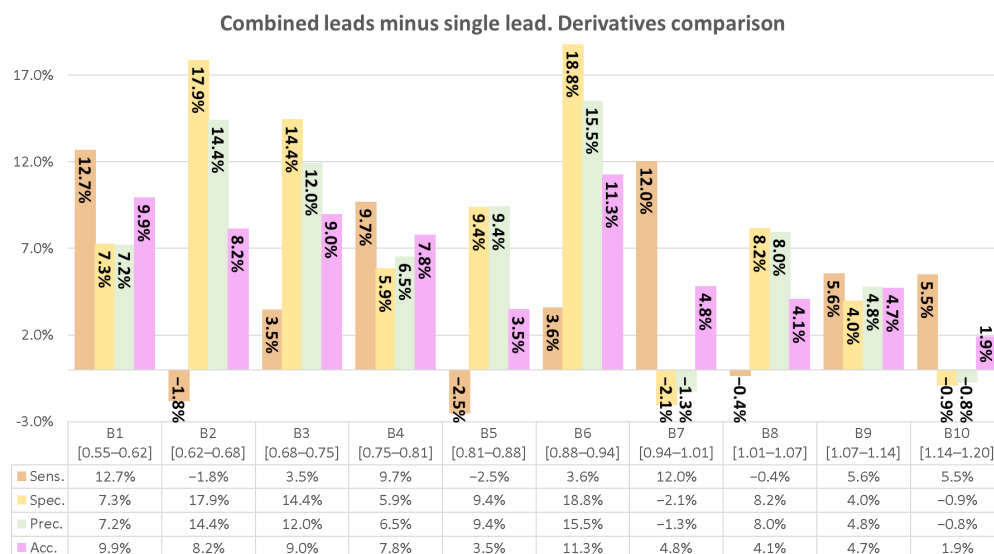


Figure 10. Combined leads classification results.



**Figure 11.** Combined leads vs. single lead: Score comparison.

In synthesis, [B1, B3, B4, B6, B9] received a direct improvement in all their derivation values. The cases of B2 and B5 are similar; both received a decrement in sensitivity of 1.8% and 2.5%, with a score of 91.0% and 86.3%; in contrast, both achieved a significant improvement in specificity and precision with values of B2:[93.4%, 93.1%] and B5:[98.9%, 98.8%], respectively. On the other hand, B7 received a decrease in specificity and precision of 2.1% and 1.3% with an equal value of 92.5% and was supported with an increase of 12% in the sensitivity with a reach of 98%. B8 achieved 94.3% in their sensitivity, which represents a decrement of 0.4%, but an increase of 8.2%, 8.0%, and 4.1% in their specificity, precision, and accuracy with final values of 94.7%, 93.2%, and 96.6%. Finally, B10 increased by 5.5% and 1.9% in the sensitivity and accuracy values to 96.5% and 95.5% and reduced by 0.9% and 0.8% in the specificity and precision with final values of 94.7% and 93.7%. We present the general classification metrics of the experiment in Table 2.

*Toward ECG Sex Recognition for Smartphone Authentication?*

The previous sections have depicted our architecture proposal and results, getting a significant classification score for ECG sex recognition, and consolidating the ECG soft-biometric sex attribute extraction. Nonetheless, there is a valid inquiry, can the ECG acquisition be exploitable and deployable to the market? The short answer is: Yes. Different companies have developed different products oriented at portable ECG analytics. All of them use Lead-I configuration and offer comfortable signal acquisition suitable to their final application. However, none of them focus on sex recognition but facilitate identification, driving risks, and health monitoring. We will make a brief of our selected products offered by AliveCor, CardioID, and NYMI (Figure 12).

In the case of heart monitoring, KardiaMobile from AliveCor generated a comfortable attachable smartphone device that helps to detect six different types of arrhythmias. Further, the functionality can be expanded with the app KardiaCare for cloud services such as periodic cardiologist revision, and secure storage, among others. This device has FDA approval, has been applied for user verification [51], and in 2020 received investments of USD 65 million from tier-1 companies, such as Qualcomm, among others [52].

CardioID, which is in the heart monitoring trade, has a deep research background and partners such as CEiiA and the multinational Bosh. Their heartbeat traceability is applied in the transportation business, embedding the leads in the truck wheel with the intention of tracking driver identity, drowsiness or fatigue detection, and cardiac pathologies [53]. In this way, upon some heart abnormality, an alert is enabled, being all linked with their central platforms. CardioID belongs to the project VALU3S (Verification and Validation of Automated Systems’ Safety and Security) sponsored by the European Union with partners

from 10 countries, Portugal, France, Germany, Czech Republic, Ireland, Italy, Spain, Sweden, and Turkey. Importantly, the CardioID acquisition technique can be applied to any other object and context, including a smartphone.

NYMI is part of the Innominds consortium; they are a startup from the University of Toronto and have developed a fully integrated workspace wearable that includes 100+ well-ranked companies such as Microsoft and Honeywell, among others [54]. NYMI is a band that validates a user into an organization for accessing control. This band has on-body detection supported by two biometrics measures: heartbeat and fingerprint. The validation works as a user identifier for company places, object manipulation, and computer session login through NFC. Depending on the user ACL, the company authorizes specific triggered options that are enabled under user presence, for example, machine ignition option or distance measuring through their Bluetooth radio.

**Table 2.** Experiment classification metrics. (Maximum values per item are in bold).

CMD	Lead	B1	B2	B3	B4	B5	B6	B7	B8	B9	B10
Acc.	X	0.809	0.841	0.853	0.864	0.892	0.813	0.904	0.927	0.915	0.936
	Y	0.743	0.802	0.811	0.811	0.852	0.851	0.890	0.892	0.883	0.924
	Z	0.803	0.826	0.830	0.869	0.889	0.821	0.866	0.926	0.910	0.924
	XY	0.870	0.893	0.871	0.889	0.896	0.920	0.856	0.943	0.955	0.937
	YZ	0.771	0.878	0.876	0.925	0.895	0.891	0.878	0.932	0.939	0.947
	XZ	0.777	0.864	0.856	0.875	0.878	0.903	0.924	0.916	0.890	0.894
	XYZ	<b>0.908</b>	<b>0.922</b>	<b>0.943</b>	<b>0.947</b>	<b>0.926</b>	<b>0.964</b>	<b>0.952</b>	<b>0.966</b>	<b>0.962</b>	<b>0.951</b>
AUC	X	0.892	0.937	0.940	0.943	0.957	0.955	0.970	0.972	0.966	0.978
	Y	0.848	0.877	0.887	0.896	0.925	0.936	0.960	0.957	0.950	0.976
	Z	0.914	0.921	0.935	0.939	0.947	0.953	0.966	0.984	0.977	0.978
	XY	0.939	0.959	0.966	0.973	0.977	0.975	0.944	0.985	0.993	0.988
	YZ	0.917	0.948	0.963	0.975	0.976	0.983	0.986	0.983	0.984	0.988
	XZ	0.923	0.939	0.939	0.951	0.960	0.956	0.978	0.964	0.955	0.950
	XYZ	<b>0.973</b>	<b>0.981</b>	<b>0.986</b>	<b>0.988</b>	<b>0.989</b>	<b>0.992</b>	<b>0.991</b>	<b>0.995</b>	<b>0.994</b>	<b>0.990</b>
Prec.	X	0.798	0.787	0.808	0.855	0.893	0.737	0.938	0.929	0.926	0.943
	Y	0.822	0.798	0.788	0.785	0.862	0.797	0.859	0.860	0.866	0.955
	Z	0.756	0.769	0.767	0.900	0.861	0.742	0.944	0.893	0.946	0.881
	XY	0.842	0.930	<b>0.949</b>	0.933	0.962	0.902	<b>0.960</b>	0.936	0.971	<b>0.958</b>
	YZ	0.705	0.873	0.816	0.896	0.842	0.828	0.805	0.934	0.949	0.957
	XZ	<b>0.912</b>	0.887	0.857	0.822	0.839	0.938	0.914	0.887	0.907	0.871
	XYZ	0.870	<b>0.931</b>	0.928	<b>0.965</b>	<b>0.988</b>	<b>0.952</b>	0.925	<b>0.973</b>	<b>0.974</b>	0.933
Sens.	X	0.832	<b>0.928</b>	0.925	0.876	0.888	0.968	0.859	0.917	0.889	0.910
	Y	0.626	0.803	0.850	0.855	0.836	0.940	0.928	0.925	0.887	0.869
	Z	0.895	0.925	0.946	0.829	0.926	0.979	0.771	<b>0.960</b>	0.857	<b>0.958</b>
	XY	0.913	0.848	0.782	0.836	0.824	0.943	0.736	0.948	0.930	0.896
	YZ	0.937	0.882	<b>0.970</b>	<b>0.961</b>	<b>0.972</b>	<b>0.986</b>	<b>0.990</b>	0.922	0.919	0.921
	XZ	0.619	0.831	0.852	0.955	0.935	0.863	0.932	0.947	0.854	0.894
	XYZ	<b>0.959</b>	0.910	0.960	0.926	0.863	0.976	0.980	0.957	<b>0.945</b>	<b>0.958</b>

Progressively, the comfort variable has been decreasing in complexity. AliveCor, CardioID, and NYMI are spearheading examples of innovative ways for capturing the ECG signals in their products. It would prepare the market for future implementations to evaluate the ECG sex classification algorithm implementation on their related devices as a soft-biometric input feature for medical decisions or user authentication.



Figure 12. Alivecor, CardioID, and NYMI product examples.

## 6. Discussion

From the perspective of our experiment, the average classification accuracy obtained was 94.4%, with peak values greater than 96% in different bins by using the Rochester database and classified with GoogLeNet, although these results are influenced by the signal quality and attributes of the database population.

The method proposed in this work congregates the time-frequency inputs of the XYZ signals in one RGB image. The literature close to this work commonly uses 12 leads and a time window of 10 s. In contrast, our approach uses a pseudo-orthogonal configuration and less signal time capture (approx. 4 s), allowing the use of fewer electrodes and fewer data. In addition, we propose to establish the heart rate dynamism as an atomic variable before any classification approach, respecting its physiological nature. Furthermore, this experiment does not control the person's position compared to close investigations that use only the resting position.

Our work and current research in this area confirm that the classification of sex with ECG signals is realizable. As a consequence, we observe that the sex property of this signal is a hidden soft biometric feature that could enrich the feature vector of an ECG identification system or areas related to health, expanding this area of study.

The projection for further research is to analyze the classification accuracy of the architecture due to the change in the heartbeat number collected. In addition, our proposal must be analyzed with a new database to evaluate the cross-validation of our model. This study invites future investigators to include the architecture proposed in their related studies and to include sex differentiation in their models. As future work for new investigations, we propose expanding the current model to apply it to a smartphone authentication context.

## 7. Conclusions

This work proposes a novel architecture that looks for the ECG sex recognition based on the pseudo-orthogonal electrode configuration using a pre-trained convolutional neural network, reaching an accuracy of  $94.4\% \pm 2.0\%$ . This result helps the design of our future work focused on the use of the sex soft-biometric attribute, evaluating its contribution in a user authentication context by ECG.

**Author Contributions:** Conceptualization, J.-L.C.L., C.P., L.G. and L.T.; methodology, J.-L.C.L. and C.P.; software, J.-L.C.L.; validation, J.-L.C.L. and C.P.; formal analysis, J.-L.C.L. and C.P.; investigation, J.-L.C.L.; resources, J.-L.C.L. and L.T.; data curation, J.-L.C.L.; writing—original draft preparation, J.-L.C.L.; writing—review and editing, J.-L.C.L. and C.P.; visualization, J.-L.C.L.; supervision, C.P.; project administration, J.-L.C.L.; funding acquisition, L.T. All authors have read and agreed to the published version of the manuscript.

**Funding:** This work was funded by the Fundacion Universitaria Compensar, the Colombian Ministry for the Information and Communications Technology (*Ministerio de Tecnologías de la Información y las Comunicaciones—MinTIC*) and the Colombian Administrative Department of Science, Technology and Innovation (*Departamento Administrativo de Ciencia, Tecnología e Innovación—Colciencias*) through the *Fondo Nacional de Financiamiento para la Ciencia, la Tecnología y la Innovación Francisco José de Caldas* (Project ID: FP44842-502-2015).

**Institutional Review Board Statement:** Not applicable.

**Informed Consent Statement:** Not applicable.

**Data Availability Statement:** The Medical Center of the University of Rochester provided the data involved in this paper. Please email the authors for guidance.

**Acknowledgments:** The authors would like to acknowledge mainly the Fundación Universitaria Compensar, including their Telecommunications Engineering Department, Research Department, English Area, and Bilingual Department, for providing time and support to complete this paper. Also to the cooperation of all partners within the *Centro de Excelencia y Apropiación en Internet de las Cosas (CEA-IoT)* project. The authors would also like to thank all the institutions that supported this work: the Colombian Ministry for the Information and Communications Technology (*Ministerio de Tecnologías de la Información y las Comunicaciones—MinTIC*) and the Colombian Administrative Department of Science, Technology and Innovation (*Departamento Administrativo de Ciencia, Tecnología e Innovación—Colciencias*) through the *Fondo Nacional de Financiamiento para la Ciencia, la Tecnología y la Innovación Francisco José de Caldas* (Project ID: FP44842-502-2015). An additional acknowledgment corresponds to Elena Wei, and Rachelle Bracha Fishbin.

**Conflicts of Interest:** The authors declare no conflict of interest.

## Abbreviations

The following abbreviations are used in this manuscript:

ADFECGDB	abdominal and direct fECG database
AF	Atrial fibrillation
ECG	Electrocardiogram
CNN	Convolutional Neural Network
DNN	Deep Neural Network
TF	Transformation
HPF	High Pass Filter
LBBB	Left Bundle Branch Block
KNN	k-nearest neighbors algorithm
LSTM	Long short-term memory
LVH	Left ventricular hypertrophy
MFF	Multimodal Feature Fusion
MIF	Multimodal Image Fusion
NSR	Normal Sinus Rhythm
PAC	Premature atrial contractions
PCLR	Patient Contrastive Learning of Representations
PTB-XL	Physikalisch-Technische Bundesanstalt
PVC	Premature ventricular contractions
RBBB	Right Bundle Branch Block
SBP	Stop Band Filter
SCP-ECG	Standard communications protocol for computer-assisted electrocardiography
SimCLR	Simple Framework for Contrastive Learning
SPAR	Symmetric Projection Attractor Reconstruction
SVEB	Supraventricular ectopic beat
SVTA	Supraventricular Tachyarrhythmia
VEB	Ventricular ectopic beat

## References

1. Hsu, Y.L.; Wang, J.S.; Chiang, W.C.; Hung, C.H. Automatic ECG-Based Emotion Recognition in Music Listening. *IEEE Trans. Affect. Comput.* **2020**, *11*, 85–99. [CrossRef]
2. Attia, Z.I.; Friedman, P.A.; Noseworthy, P.A.; Lopez-Jimenez, F.; Ladewig, D.J.; Satam, G.; Pellikka, P.A.; Munger, T.M.; Asirvatham, S.J.; Scott, C.G.; et al. Age and Sex Estimation Using Artificial Intelligence From Standard 12-Lead ECGs. *Circ. Arrhythmia Electrophysiol.* **2019**, *12*, e007284. [CrossRef]
3. Cabra, J.L.; Mendez, D.; Trujillo, L.C. Wide Machine Learning Algorithms Evaluation Applied to ECG Authentication and Gender Recognition. In Proceedings of the 2nd International Conference on Biometric Engineering and Applications (ICBEA), Amsterdam, The Netherlands, 16–18 May 2018; pp. 58–64.
4. Siegersma, K.; Van De Leur, R.; Onland-Moret, N.C.; Van Es, R.; Den Ruijter, H.M. Misclassification of sex by deep neural networks reveals novel ECG characteristics that explain a higher risk of mortality in women and in men. *Eur. Heart J.* **2021**, *42*, 3162. [CrossRef]
5. Nguyen, D.T.; Kim, K.W.; Hong, H.G.; Koo, J.H.; Kim, M.C.; Park, K.R. Gender Recognition from Human-Body Images Using Visible-Light and Thermal Camera Videos Based on a Convolutional Neural Network for Image Feature Extraction. *Sensors* **2017**, *17*, 637. [CrossRef] [PubMed]
6. Ghildiyal, A.; Sharma, S.; Verma, I.; Marhatta, U. Age and Gender Predictions using Artificial Intelligence Algorithm. In Proceedings of the 3rd International Conference on Intelligent Sustainable Systems (ICISS'20), Thoothukudi, India, 3–5 December 2020; pp. 371–375.
7. Lee, M.; Lee, J.H.; Kim, D.H. Gender recognition using optimal gait feature based on recursive feature elimination in normal walking. *Expert Syst. Appl.* **2022**, *189*, 116040. [CrossRef]
8. Alkhalwaldeh, R.S. DGR: Gender Recognition of Human Speech Using One-Dimensional Conventional Neural Network. *Sci. Program.* **2019**, *2019*, 7213717. [CrossRef]
9. Ikae, C.; Savoy, J. Gender identification on Twitter. *J. Assoc. Inf. Sci. Technol.* **2021**, *73*, 58–69. [CrossRef]
10. Tsimperidis, I.; Yucel, C.; Katos, V. Age and Gender as Cyber Attribution Features in Keystroke Dynamic-Based User Classification Processes. *Electronics* **2021**, *10*, 835. [CrossRef]
11. Bayer. Las Enfermedades Cardiovasculares son la Primera Causa de Muerte en Colombia y el Mundo. 2020. Available online: <https://www.bayer.com/es/co/las-enfermedades-cardiovasculares-son-la-primera-causa-de-muerte-en-colombia-y-el-mundo> (accessed on 28 April 2022).
12. Centers for Disease Control and Prevention. Heart Disease Facts. 2022. Available online: <https://www.cdc.gov/heartdisease/facts.htm> (accessed on 28 April 2022).
13. Publishing, H.H. The Heart Attack Gender Gap. 2016. Available online: <https://www.health.harvard.edu/heart-health/the-heart-attack-gender-gap> (accessed on 28 April 2022).
14. Health, H. Throughout Life, Heart Attacks are Twice as Common in Men than Women—Harvard Health. 2016. Available online: <https://www.health.harvard.edu/heart-health/throughout-life-heart-attacks-are-twice-as-common-in-men-than-women> (accessed on 28 April 2022).
15. Albrektsen, G.; Heuch, I.; Løchen, M.L.; Thelle, D.S.; Wilsgaard, T.; Njølstad, I.; Bønaa, K.H. Lifelong Gender Gap in Risk of Incident Myocardial Infarction: The Tromsø Study. *JAMA Intern. Med.* **2016**, *176*, 1673–1679. [CrossRef]
16. Cho, L. Women or Men—Who Has a Higher Risk of Heart Attack? 2020. Available online: <https://health.clevelandclinic.org/women-men-higher-risk-heart-attack/> (accessed on 28 April 2022).
17. Mieszczanska, H.; Pietrasik, G.; Piotrowicz, K.; McNitt, S.; Moss, A.J.; Zareba, W. Gender Related Differences in Electrocardiographic Parameters and Their Association with Cardiac Events in Patients After Myocardial Infarction. *Am. J. Cardiol.* **2008**, *101*, 20–24. [CrossRef] [PubMed]
18. Nakagawa, M.; Ooie, T.; Ou, B.; Ichinose, M.; Yonemochi, H.; Saikawa, T. Gender differences in the dynamics of terminal T wave intervals. *Pacing Clin. Electrophysiol.* **2004**, *27*, 769–774. [CrossRef] [PubMed]
19. Ergin, S.; Uysal, A.K.; Gunal, E.S.; Gunal, S.; Gulmezoglu, M.B. ECG based biometric authentication using ensemble of features. In Proceedings of the 9th Iberian Conference on Information Systems and Technologies (CISTI'14), Barcelona, Spain, 18–21 June 2014; pp. 1274–1279.
20. Pinto, J.R.; Cardoso, J.S.; Lourenço, A. Evolution, Current Challenges, and Future Possibilities in ECG Biometrics. *IEEE Access* **2018**, *6*, 34746–34776. [CrossRef]
21. Jain, A.K.; Nandakumar, K.; Lu, X.; Park, U. Integrating Faces, Fingerprints, and Soft Biometric Traits for User Recognition. In Proceedings of the 2nd Biometric Authentication ECCV International Workshop (BioAW'04), Prague, Czech Republic, 15 May 2004; Springer: Berlin/Heidelberg, Germany 2004; pp. 259–269.
22. Ceci, M.; Japkowicz, N.; Liu, J.; Papadopoulos, G.A.; Raś, Z.W. Foundations of Intelligent Systems. In *Proceedings of the 24th International Symposium, ISMIS 2018, Limassol, Cyprus, 29–31 October 2018*, Springer: Cham, Switzerland, 2018; pp. 120–129.
23. Roy, A.; Memon, N.; Ross, A. MasterPrint: Exploring the Vulnerability of Partial Fingerprint-Based Authentication Systems. *IEEE Trans. Inf. Forensics Secur.* **2017**, *12*, 2013–2025. doi: [CrossRef]
24. Winder, D. Hackers Claim 'Any' Smartphone Fingerprint Lock Can be Broken in 20 Minutes. Available online: <https://www.forbes.com/sites/daveywinder/2019/11/02/smartphone-security-alert-as-hackers-claim-any-fingerprint-lock-broken-in-20-minutes/?sh=2ca0734f6853> (accessed on 15 June 2022).

25. Mott, N. Hacking Fingerprints Is Actually Pretty Easy—And Cheap. 2021. Available online: <https://www.pcmag.com/news/hacking-fingerprints-is-actually-pretty-easy-and-cheap> (accessed on 15 June 2022).
26. Winder, D. Apple's iPhone FaceID Hacked In Less Than 120 Seconds. 2019. Available online: <https://www.forbes.com/sites/daveywinder/2019/08/10/apples-iphone-faceid-hacked-in-less-than-120-seconds/?sh=349627621bc3> (accessed on 15 June 2022).
27. Pato, J.; Millett, L. *Biometric Recognition: Challenges and Opportunities*, 1st ed.; The National Academies Press: Washington, DC, USA, 2010; p. 165.
28. Atkielski, A. Schematic Diagram of Normal Sinus Rhythm for a Human Heart as Seen on ECG. 2009. Available online: <https://commons.wikimedia.org/wiki/File:SinusRhythmLabels-es.svg> (accessed on 25 June 2022).
29. İzci, E.; Değirmenci, M.; Özdemir, M.A.; Akan, A. ECG Arrhythmia Detection with Deep Learning. In Proceedings of the 28th IEEE Signal Processing and Communications Applications (SIU), Gaziantep, Turkey, 5–7 October 2020; pp. 1541–1544.
30. Essa, E.; Xie, X. An Ensemble of Deep Learning-Based Multi-Model for ECG Heartbeats Arrhythmia Classification. *IEEE Access* **2021**, *9*, 103452–103464. [[CrossRef](#)]
31. Ahmad, Z.; Tabassum, A.; Guan, L.; Khan, N.M. ECG Heartbeat Classification Using Multimodal Fusion. *IEEE Access* **2021**, *9*, 100615–100626. [[CrossRef](#)]
32. Niu, J.; Tang, Y.; Sun, Z.; Zhang, W. Inter-Patient ECG Classification With Symbolic Representations and Multi-Perspective Convolutional Neural Networks. *IEEE J. Biomed. Health Inform.* **2020**, *24*, 1321–1332. [[CrossRef](#)]
33. Ebrahimi, Z.; Loni, M.; Daneshlab, M.; Gharehbaghi, A. A review on deep learning methods for ECG arrhythmia classification. *EXpert Syst. Appl. X* **2020**, *7*, 100033. [[CrossRef](#)]
34. Bahrami, M.; Forouzanfar, M. Sleep Apnea Detection From Single-Lead ECG: A Comprehensive Analysis of Machine Learning and Deep Learning Algorithms. *IEEE Trans. Instrum. Meas.* **2022**, *71*, 1–11. [[CrossRef](#)]
35. Lee, K.J.; Lee, B. End-to-End Deep Learning Architecture for Separating Maternal and Fetal ECGs Using W-Net. *IEEE Access* **2022**, *10*, 39782–39788. [[CrossRef](#)]
36. Li, H.; Deng, J.; Feng, P.; Pu, C.; Arachchige, D.D.K.; Cheng, Q. Short-Term Nacelle Orientation Forecasting Using Bilinear Transformation and ICEEMDAN Framework. *Front. Energy Res.* **2021**, *9*, 780928. [[CrossRef](#)]
37. Li, H.; Deng, J.; Yuan, S.; Feng, P.; Arachchige, D.D.K. Monitoring and Identifying Wind Turbine Generator Bearing Faults Using Deep Belief Network and EWMA Control Charts. *Front. Energy Res.* **2021**, *9*, 799039. [[CrossRef](#)]
38. Gajare, A.; Dey, H. MATLAB-based ECG R-peak Detection and Signal Classification using Deep Learning Approach. In Proceedings of the 3rd IEEE Bombay Section Signature Conference (IBSSC), Gwalior, India, 18–20 November 2021; pp. 157–162.
39. Cai, W.; Hu, D. QRS Complex Detection Using Novel Deep Learning Neural Networks. *IEEE Access* **2020**, *8*, 97082–97089. [[CrossRef](#)]
40. Pokaprakarn, T.; Kitzmiller, R.R.; Moorman, R.; Lake, D.E.; Krishnamurthy, A.K.; Kosorok, M.R. Sequence to Sequence ECG Cardiac Rhythm Classification Using Convolutional Recurrent Neural Networks. *IEEE J. Biomed. Health Inform.* **2022**, *26*, 572–580. [[CrossRef](#)] [[PubMed](#)]
41. Abdeldayem, S.S.; Bourlai, T. A Novel Approach for ECG-Based Human Identification Using Spectral Correlation and Deep Learning. *IEEE Trans. Biom. Behav. Identity Sci.* **2020**, *2*, 1–14. [[CrossRef](#)]
42. Uwaechia, A.N.; Ramli, D.A. A Comprehensive Survey on ECG Signals as New Biometric Modality for Human Authentication: Recent Advances and Future Challenges. *IEEE Access* **2021**, *9*, 2169–3536. [[CrossRef](#)]
43. Strodtzoff, N.; Wagner, P.; Schaeffter, T.; Samek, W. Deep Learning for ECG Analysis: Benchmarks and Insights from PTB-XL. *IEEE J. Biomed. Health Inform.* **2021**, *25*, 1519–1528. [[CrossRef](#)]
44. Siegersma, K.R.; van de Leur, R.R.; Onland-Moret, N.C.; Leon, D.A.; Diez-Benavente, E.; Rozendaal, L.; Bots, M.L.; Coronel, R.; Appelman, Y.; Hofstra, L.; et al. Deep neural networks reveal novel sex-specific electrocardiographic features relevant for mortality risk. *Eur. Heart J.-Digit. Health* **2022**, *3*, 1–10. [[CrossRef](#)]
45. Chen, T.; Kornblith, S.; Norouzi, M.; Hinton, G. A Simple Framework for Contrastive Learning of Visual Representations. In Proceedings of the 37th International Conference on Machine Learning (ICML'20), Vienna, Austria, 12–18 July 2020; pp. 1597–1607.
46. Diamant, N.; Reinertsen, E.; Song, S.; Aguirre, A.D.; Stultz, C.M.; Batra, P. Patient contrastive learning: A performant, expressive, and practical approach to electrocardiogram modeling. *PLoS Comput. Biol.* **2022**, *18*, e1009862. [[CrossRef](#)]
47. Lyle, J.V.; Nandi, M.; Aston, P.J. Symmetric Projection Attractor Reconstruction: Sex Differences in the ECG. *Front. Cardiovasc. Med.* **2021**, *8*, 1–17. [[CrossRef](#)]
48. brgfx. Telemetric and ECG Holter Warehouse Project. Available online: <http://thew-project.org/Database/E-HOL-03-0202-003.html> (accessed on 18 June 2022).
49. brgfx. Vector de Cuerpo Humano Creado por Brgfx - www.freepik.es. 2021. Available online: <https://www.freepik.es/vectores/cuerpo-humano> (accessed on 18 June 2022).
50. Padsalgikar, A. *Plastics in Medical Devices for Cardiovascular Applications. A Volume in Plastics Design Library*, 1st ed.; Elsevier: Kidlington, UK, 2017; p. 115.
51. Arteaga-Falconi, J.S.; Osman, H.A.; Saddik, A.E. ECG Authentication for Mobile Devices. *IEEE Trans. Instrum. Meas.* **2016**, *65*, 591–600. [[CrossRef](#)]
52. Wiggers, K. AliveCor Raises \$65 Million to Detect Heart Problems with AI. 2020. Available online: <https://venturebeat.com/2020/11/16/alivecor-raises-65-million-to-detect-heart-problems-with-ai/> (accessed on 28 October 2021).

53. CardioID. Every Heart Has a Beat, But the Way We Use it is Unique! 2016. Available online: <https://www.cardio-id.com/> (accessed on 28 October 2021).
54. Nymi. Nymi Workplace Wearables. 2021. Available online: <https://www.nymi.com/nyimi-band> (accessed on 28 October 2021).